Int. J. Electrochem. Sci., 14 **(2019)** 9726 – 9740, doi: 10.20964/2019.10.25

International Journal of
ELECTROCHEMICAL
SCIENCE
www.electrochemsci.org

Corrosion Inhibition Effect of Sodium Pyrophosphate on Carbon Steel in Chloride Contaminated Mortar

Yiwen Xu[1], *Chao Zhu*[1], *Shengli Chen*[3], *Yiji Zhang*[1], *Tong Wu*[1], *Xiangyu Lu*[1,2,*], *Mai Wang*[4], *Xingguo Feng*[1,2]

[1] Jiangsu Key Laboratory of Coast Ocean Resources Development and Environment Security, Hohai University, Nanjing 210098, Jiangsu, China
[2] State Key Laboratory of Geohazard Prevention and Geoenvironment Protection, Chengdu University of Technology, Chendu 610059, Sichuan, China
[3] CNOOC information technology Co., Ltd. Oceanographic information Center, Beijing 100013, China
[4] Air Force Command College, Beijing 100089, China
[*]E-mail: luxiangyu@hhu.edu.cn

Received: 5 June 2019 / *Accepted:* 4 August 2019 / *Published:* 30 August 2019

Reinforced concrete structures suffered severe degradation for the corrosion of the steel bar, and the utilization of phosphate corrosion inhibitors was an eco-friendly as well as an effective method to reduce the steel corrosion. Sodium pyrophosphate (SPP) was used to inhibit the corrosion of the steel bar in the chloride contaminated mortar. The corrosion behavior of the rebar in mortars containing different concentrations of SPP was investigated via electrochemical tests. The results showed that the SPP can efficiently hinder the corrosion of the rebar in the chloride-containing mortars. In the samples containing SPP with a concentration of 0.6% by the weight of cement, the corrosion of rebar was most effectively inhibited. The excessive addition of SPP could cause the degradation of mortar cover layer and reduce its inhibition efficiency.

Keywords: corrosion inhibitor; sodium pyrophosphate; mortar; carbon steel; electrochemical tests

1. INTRODUCTION

The degradation of steel-reinforced concrete mainly caused by chloride ion in aggressive environment, which accelerates the corrosion of reinforcing steel in the structures [1-3]. The utilization of the corrosion inhibitor was thought to be an effective way to hinder the reinforcement corrosion [4]. Although the nitrites, especially $Ca(NO_2)_2$, have been used in concrete as the corrosion inhibitor for decades, its high dosage, toxicity, as well as the negative effect on the workability of concrete was reported, and it was gradually limited to utilizing in many countries [5-7]. Therefore, the development

of the newly efficient and eco-friendly corrosion inhibitors for steel rebar is one of the candidate ways to overcome the durability issue of concrete structures.

Phosphate-based inhibitors for reinforcing steel attracted many attentions from the scientists recently. Earlier studies [8-10] had confirmed that the phosphate-based inhibitors could react with the calcium ions in cement paste and form insoluble substances, which increases the compactness and reduces the permeability of concrete. Alonso [11] investigated the inhibition effect of sodium monofluorophosphate (Na_2PO_3F) on the corroded steel in the carbonated concrete. The corrosion rate of the corroded rebar was significantly diminished, while the corrosion potential was obviously positively shifted, which indicates that the Na_2PO_3F (MFP) is an anodic inhibitor. The authors attributed its inhibition effect to the formation of orthophosphate and fluoride during the hydrolysis process in the neutral media. Chaussadent [12] and Iglesia [13] further investigated the inhibition mechanism of MFP in mortars and found that the MFP reacted with portlandite, formed hydroxyfluoroapatite and more OH^-, which benefits the passivation of steel. Shi and Sun [5, 14] investigated the inhibition efficiency of Na_3PO_4 (TSP) and sodium nitrite ($NaNO_2$) on reinforcing steel in the mortars and the saturated $Ca(OH)_2$ solutions, respectively. The results suggested that the nitrite more effectively reduced the uniform corrosion than the phosphate in the two conditions, while the former inhibitor more effectively prevented the pitting corrosion on the carbon steel than the former one. Moreover, the authors proposed that the TSP is a cathodic inhibitor for its dual protective effect on the reinforced steel [14]: (a) the depositions of $Ca_3(PO_4)_2$ formed during the reaction between phosphate and hydration products block the mortar micro-structure; (b) the phosphate reacts with steel, forming a protective layer against the chloride-induced damage. Yohai and co-authors [15] studied the inhibitive properties of TSP on steel in the chloride-containing mortars, and the results indicated that the TSP hinders the corrosion of rebar and presents a mix-type inhibitor in the mortars. The authors also ascribed the inhibitive effect to the presence of $Ca_3(PO_4)_2$ and the absorbed layer, which blocks the pores and inhibits the corrosion of the reinforcing steel, respectively [16]. Bastidas and co-authors [17, 18] compared the inhibition effect of three phosphates (Na_2PO_3F, Na_2HPO_4, Na_3PO_4) on the carbon steel in mortar. The authors suggested that all the three phosphates could be categorized as anodic corrosion inhibitors, and the MFP presented the highest inhibitive efficiency, while the TSP showed the lowest. In general, the corrosion inhibition efficiency of phosphates had been extensively investigated [5, 8-18], but some contradictory conclusions [14-18] were reported. Then, further study should be carried out to investigate the corrosion inhibition behavior of the phosphate-based inhibitors.

Sodium pyrophosphate (SPP) has the commonality of the phosphates and a better complexing ability for one more phosphorus-oxygen tetrahedron than TSP. It can perform as an efficient corrosion inhibitor in cooling water treatment system [19]. The studies about the inhibition behavior of SPP on steel are mostly conducted in the chloride-containing solution [19, 20]. For instance, Chen [19] studied the protective effect of SPP on the steel bar in a simulated concrete pore solution. The results suggested that the addition of SPP leads to the positive shift in corrosion potential of the steel, which suggested that the SPP was an anodic inhibitor in concrete pore solution. The inhibition efficiency on the reinforcing steel was enhanced when the addition of SPP increased, which could reach 97.5% as the concentration of SPP was 0.03 mol/L. Etteyeb [20] compared the inhibition efficiency of Na_3PO_4, $Na_4P_2O_7$ and $C_2H_8O_7P_2$ on the carbon steel in the alkaline solution. The authors found that the corrosion

rate of the steel bar in alkaline solution with SPP is the lowest, but that of the one in the solution with TSP is the highest. Actually, the inhibition mechanisms of the phosphates in the mortars or concrete were more complex than that in the simulated solutions. In the present work, the corrosion inhibition of sodium pyrophosphate on the carbon steel in chloride contaminated mortars was investigated via different electrochemical tests. The results suggested that SPP can efficiently hinder the corrosion of rebar in the chloride contaminated mortars, but the excessive addition of SPP could decrease its inhibition efficiency owing to the degradation of concrete cover layer.

2. MATERIALS AND EXPERIMENTS

2.1 Materials

Q235 steel rod, with the chemical composition (wt.%): carbon 0.37%, silicon 0.16%, manganese 0.32%, sulphur 0.053%, phosphorus 0.026% and iron for the balance, was used in the present study. Plain ground steel rods (Φ 10mm) were cut into 5 mm and 50 mm, used in the simulated concrete pore solution and the chloride contaminated mortar, respectively. Prior to the tests, the steel samples were ground with alumina sandpapers up to grade 600, and then were washed with deionized water and degreased with anhydrous ethanol. The steel samples used in the simulated pore solution were further ground up to grade 1500, and then were polished by using a MP-1B automatic metallographic grinder (Bingyu, China) at a spin rate of 300 rpm. The polished surface was rinsed with anhydrous ethanol before immersion in simulated concrete pore solution. The steel samples were welded with copper wires at one end for the electrochemical measurements. The welding cross section was covered with silicone coating, leaving a testing area of 16.5 cm^2.

Ordinary Portland cement (P.O 42.5) and river sand were used for preparing the cylindrical mortar at a mixed ratio of 1:3, with water/cement ratio of 0.65. Sodium chloride (3.0% (wt.%)) was added into the mixing water to accelerate the corrosion of steel bars. The longer steel bars were embedded in the cylindrical mortar with a size of Φ 40×60 mm. SPP with different weight ratios of cement, including 0%, 0.3%, 0.6%, 1.2%, and 2.4%, were mixed into the mortars to study its inhibition efficiency. Mortar cubes containing different concentrations of SPP with size of 70 × 70 × 70 mm were casted for compressive strength testing. Five parallel mortar samples were prepared for each SPP concentration. All the mortar samples were immersed in a 3.5% NaCl solution. Saturated calcium hydroxide solutions were adopted to simulate the concrete pore solution [21-23], and different concentrations of SPP, including 0 mol/L, 6.75×10^{-3} mol/L, 1.35×10^{-2} mol/L, 2.70×10^{-2} mol/L, and 5.40×10^{-2} mol/L were added to investigate its inhibitor behavior. After immersed 48 h in the chloride-containing pore solution with different concentration of SPP, the surface of steel was examined by the scanning electron microscope (SEM).

2.2 Experiments

Electrochemical measurements, including open-circuit potential (OCP), electrochemical impedance spectroscopy (EIS), and linear polarization resistance (LPR) were carried out to study the

inhibition efficiency of SPP on the carbon steel in the chloride contaminated mortars. All the electrochemical tests were conducted with a CS350 electrochemical workstation (Corrtest instrument, China), using a classical three-electrode system: a testing carbon steel sample, a platinum electrode, and a saturated calomel electrode (SCE) were connected to the working, counter, and reference electrodes, respectively. OCP of the steel samples in the mortars was recorded every 5 days. According to earlier studies, the LPR measurements were performed at ±10 mV vs OCP at a scan rate of 0.1666 mV/s [24-26], after the OCP tests. The EIS tests were conducted at OCP in the range from 10^5 to 10^{-2} Hz with an AC disturbance signal of 10 mV every 10 days. At an interval of 30 days, potentiodynamic polarization curves of the steel samples in the mortars with different contents of SPP were tested at a scan rate of 1mV/s in the range of -0.3~1.5 V vs OCP [27, 28]. According to the Tafel extrapolation method [29], the corrosion parameters of the carbon steel samples were obtained by fitting the potentiodynamic polarization curves, using the Corrview software (Scribner, Inc). At 90 days, the mortar cover layer was removed to observe the corrosion state of the reinforcing steel. For the steel samples immersed in the chloride-containing pore solutions, the surface of the steel was examined by using a Hitachi S-3400N scanning electron microscope. The compressive strengths of the mortar cubes containing different contents of SPP were measured at 14 days with a SHT4305 universal testing machine (Kason, China), according to standard ASTM C349 [30].

3. RESULTS AND DISCUSSION

3.1. Open-circuit potential

Figure 1 represents the variation of OCP of the steel bars in the chloride contaminated mortar with different content of SPP. The results show that the OCP values negatively shifted in initial several days, and reached a relative stability stage after 60 days. Furthermore, as being compared with the OCP values of the samples in chloride contaminated mortar without SPP, those of the samples in SPP-containing mortar are obviously higher, which indicates that the addition of SPP could reduce the risk of corrosion for the steel bars in chloride contaminated mortar. In an early study, Grover [31] proposed that the pyrophosphate could hydrolyze and form orthophosphate in the concrete environment. Thus, the increase of OCP could be related to the insoluble pyrophosphate compounds blocking the mortar micro-pores and hinder the penetration of chloride from the solution. Similarly, Shi et al. [14] reported that the OCP of rebar evidently increased after adding phosphates into the mortars. Moreover, in the mortar with 0.6% SPP, the OCP values of steel samples are the highest. When the content of SPP exceeds 0.6%, the values of OCP decreased with the content of SPP in the mortars. This situation suggests that the inhibition efficiency presented the highest values in the mortar with 0.6% SPP, and the further increase in the content of SPP could reduce its inhibition effect.

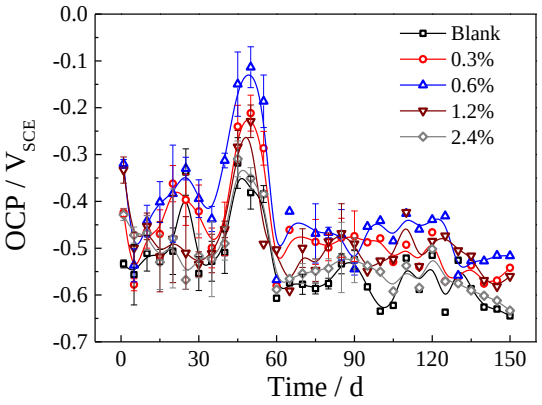

Figure 1. Open-circuit potential of steel samples in the Cl^- contaminated mortars with time and SPP content.

3.2. Linear polarization resistance

The polarization resistance (R_p) is widely used to assess the corrosion rate of steel bars in mortar, which can be obtained from the linear polarization curves, according to Eq. (1) [32]. The corrosion current density (i_{corr}) is related to R_p by the Stern-Geary constant (B), as shown in Eq. (2) and (3) [5, 20, 33].

$$R_p = \left(\frac{\partial \Delta E}{\partial i}\right)_{i=0, dE/dt \to 0} \quad (1)$$

$$i_{corr} = \frac{B}{R_p} \quad (2)$$

$$B = \frac{\beta_a \beta_c}{2.303(\beta_a + \beta_c)} \quad (3)$$

where E is the applied potential around the OCP, i_{corr} is the corrosion current density, β_a and β_c are the anodic and cathodic Tafel slopes, respectively. Based on the results in previous studies [34-36], the β_a and β_c of carbon steel rebar in concrete is 90 mV/dec and -180 mV/dec, respectively. Thus, the Stern-Geary constant (B) value of 26 mV/dec was used here, which had been confirmed that it was appropriate for active state steel embedded in concrete [35]. The polarization resistance (R_p) and the corresponding corrosion current density (i_{corr}) are presented in figure. 2. As figure 2a shows, the R_p of steel bar in mortar sharply decreases with time in the initial 10 days, and maintains at a relatively stable stage after 60 days, which is similar to the results of OCP (figure 1). The order of the magnitude of i_{corr} (figure 2b) is 0.01~1 μA cm^{-2}, and almost increases by two orders of magnitude during the experiment period. Bastidas [17] reported a similar magnitude of i_{corr} for steel bars embedded in mortar containing 3% sodium phosphates as corrosion inhibitors. Furthermore, the R_p and i_{corr} of steel bars in mortar without SPP are the lowest and the highest, respectively, in comparing with those of the steel bars in the SPP-containing mortars. The results indicate that the addition of SPP could hinder the corrosion of the rebars in the chloride contaminated mortars. Moreover, the steel bars in mortar containing 0.6% SPP have the lowest i_{corr} values, as low as less than 0.2 μA cm^{-2} during the whole experiment period. Alonso [11] categorized this scenario (< 0.2 μA cm^{-2}) to the passive state, indicating a relatively low risk of corrosion. The i_{corr} of steel bars in mortar with 0.6% SPP are ~ 40% of those in the blank samples, which

means that the addition of 0.6% SPP by weight of cement can hinder 60% corrosion of steel bars. However, the further increase of SPP content diminishes the value of R_p and increases the i_{corr}, then its inhibition efficiency on steel bars is reduced. The situation is in line with the open-circuit potential results (figure 1), which indicates that the highest inhibition efficiency on the carbon steel was in the mortar with 0.6% SPP, and excessive addition of SPP could cause the efficiency diminish.

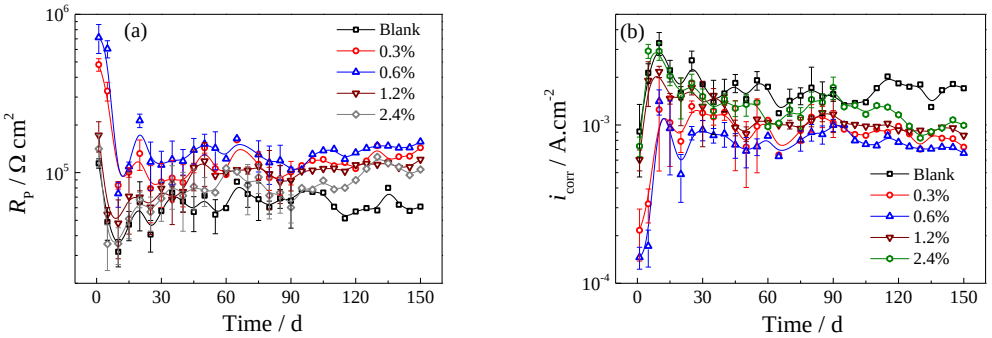

Figure 2. Variation of (a) polarization resistance and (b) corrosion current density of carbon steel bars with time and SPP contents.

3.3. Electrochemical impedance spectroscopy

The EIS results of carbon steel bars in the chloride contaminated mortar with various contents of SPP were tested at 1, 30, 60, 90 and 120 days, and the results are presented in figure 3. Two arcs can be observed in Nyquist plots, the radius of the capacitive loop for sample in mortar containing SPP increases with time, indicating the gradually passivation of the carbon steel samples. Simultaneously, for a given immersion time, the impedance values (figure 4) of steel bars in the SPP-containing mortar are significantly higher than those of the ones in mortar without SPP. The highest impedance value is observed on the steel samples in the mortar with 0.6% SPP, while the impedance values of samples diminished when the content of the SPP exceeds 0.6%. The EIS results, together with the OCP (figure 1) and the R_p (figure 2) results, suggesting that the SPP significantly inhibition the corrosion of carnon steel rebars in the chloride contaminated mortar, and the most suitable content of SPP is 0.6% by weight of cement.

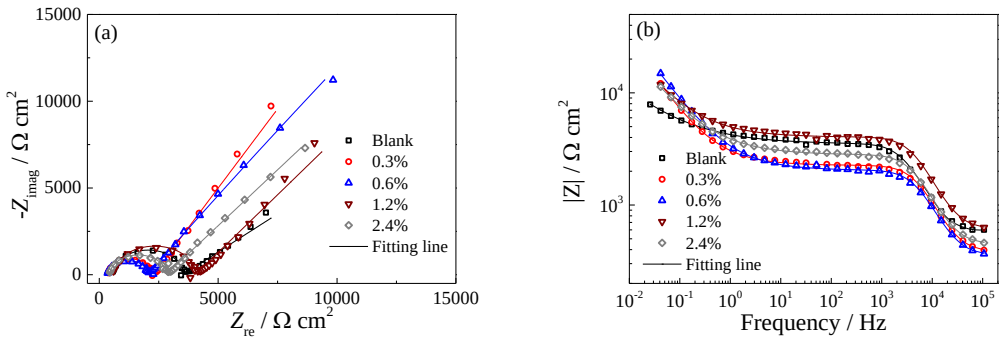

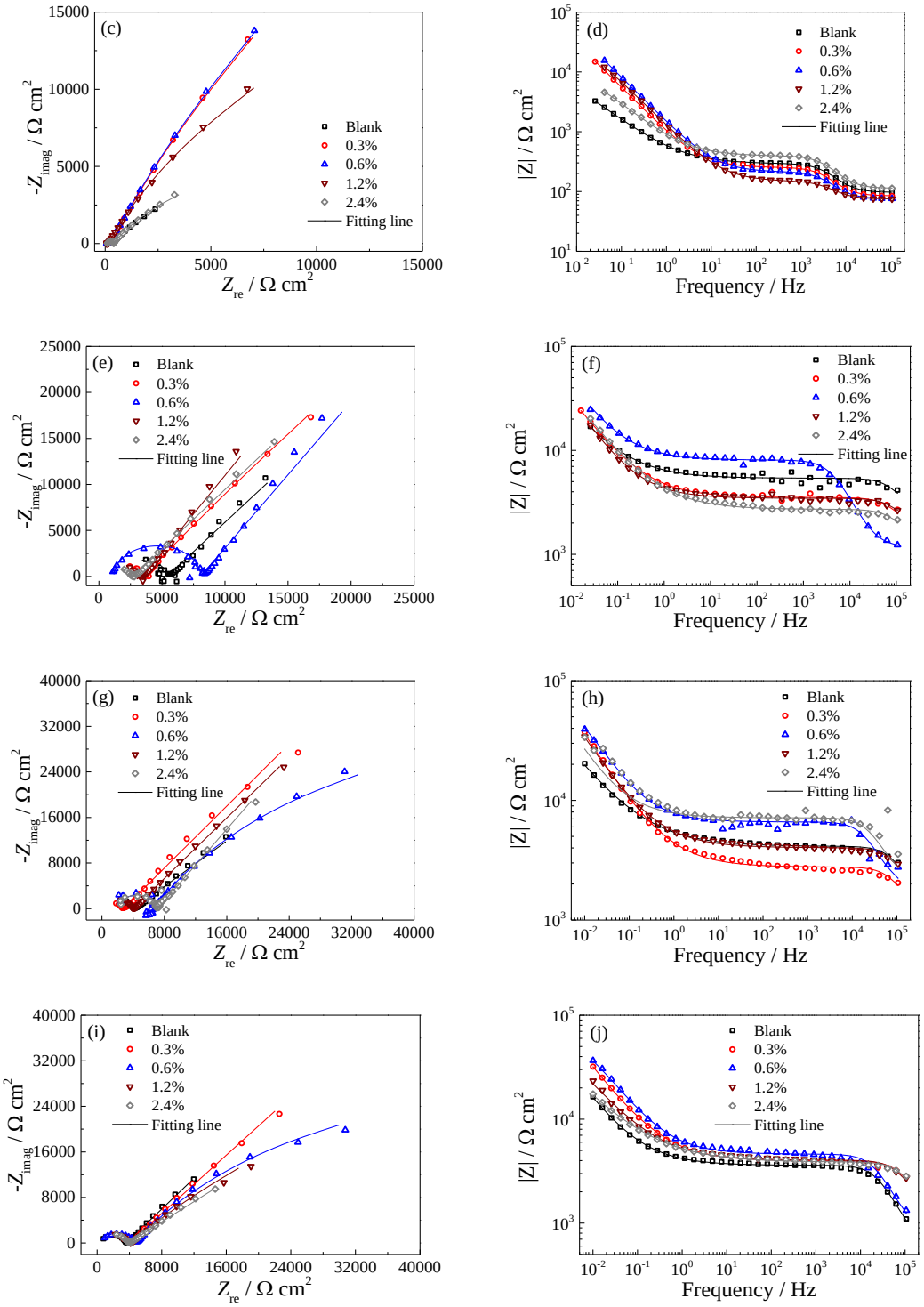

Figure 3. Nyquist and Bode plots of carbon steel bars in the chloride contaminated mortar with different contents of SPP at different immersion time. (a) and (b) 1 day, (c) and (d) 30 days, (e) and (f) 60 days, (g) and (h) 90 days, (i) and (j) 120 days.

An equivalent circuit (figure 5) is used to fit the EIS results, by applying the Zsimpwin software [37-39]. As Figure 3 shows, excellent fit between the experimental data and calculated results was observed. The parameters of the circuit component are defined as follow: R_s is the resistance of the electrolyte; Q_c and R_c are the capacitance and resistance of the mortar cover layer, respectively; R_{ct}

represents the polarization resistance of the steel/mortar interface, and the Q_{dl} is the double layer capacitance [5, 40]. The Q_{dl}, equivalent to the C_d, which is related to the thickness of film, can be calculated by the following formulas [41, 42]:

$$C_d = Y_0(\omega_{MAX})^{n-1} \quad (4)$$

$$C_d = \frac{\varepsilon\varepsilon_0 S}{d} \quad (5)$$

where Y_0 and n are associated with the surface electroactivity and the constant phase element exponent, respectively, which both can be directly obtained from the fitted results. ω_{MAX} equals to 0.025 Hz, is the frequency at the maximum $-Z_{imag}$ in the Nyquist plot. ε and ε_0 are the dielectric constants of the vacuum and the passive film. S and d are the passive film area and double-layer thickness, respectively.

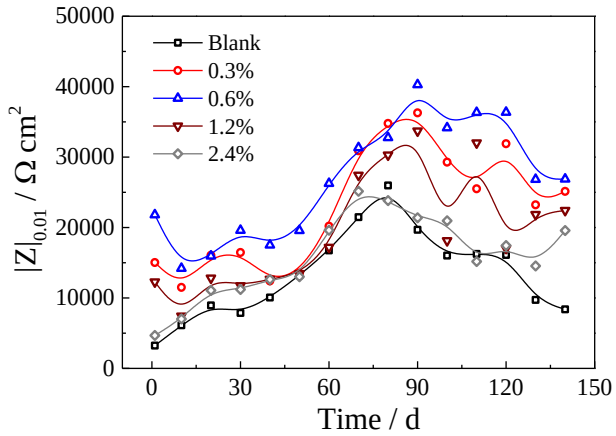

Figure 4. Variation of low-frequency (0.01 Hz) impedance values of carbon steel bars in chloride contaminated mortar with different content of SPP.

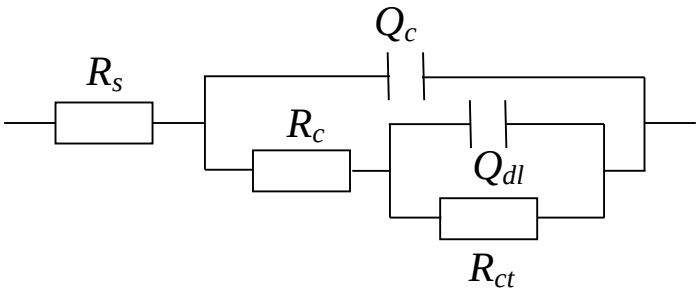

Figure 5. Equivalent circuit applied to fit the EIS results of the rebars in the chloride contaminated mortars.

The EIS fitted results of the rebars in chloride contaminated mortar are presented in Figure 6. Clearly, the R_{ct} is nearly one orders of magnitude larger than the R_c, which is similar to the results reported by Morris [43]. By analyzing the EIS data with an equivalent circuit containing elements of concrete resistance (R_s) and polarization resistance (R_p), the authors also found that the former resistance is much lower than the latter one. In the present study, it easy to notice that the values of R_{ct} decreased with immersion time and maintained at a relatively stable stage after 90 days, which is similar to the trend of

R_p from the LPR measurement (figure 2a). Simultaneously, the fitted polarization resistance (R_p) of steel bars in the blank mortar (without SPP) is evident lower than those of the rebars in the SPP-containing mortars. Moreover, the steel samples in the mortars with 0.6% (wt.%) SPP presented the highest R_{ct}, and the values of R_{ct} decreased with the contents of SPP when it exceeds 0.6%. On the contrary, the double layer capacitance Q_{dl} (figure 6c) decreases with the concentration of SPP in chloride contaminated mortar. According to Eq. (5), this situation indicates that a protective layer formed on the steel surface by addition of SPP, and the thickness of the films increases with the concentration of SPP in the chloride contaminated mortar, suggesting that the protection of the absorbed layer is enhanced with increasing SPP concentration. The scenario that the inhibition efficiency of SPP decreases with its concentration when it exceeds 0.6% by weight of cement will further discussion in the following.

As shown in Figure 6a, the R_c of mortar containing SPP is relatively lower than that of mortar without SPP at the initial stage. In fact, previous studies [31, 44, 45] have reported that the pyrophosphates in mortars could combine with the surface of newly forming crystals, thus can be applied as retarder to inhibit the crystallization and increase the setting time of the concrete, which has the best retarding effect among the phosphates. Therefore, the lower R_c of the SPP-containing mortars could be attributed to the incomplete solidification of mortars. As immersion time prolongs, the formation of phosphate products blocks the mortar micropores, then the permeability of mortar is reduced, and the R_c of mortar containing SPP becomes larger than that of mortar without SPP. Interestingly, the R_c of mortar decrease with the content of SPP when its addition exceeds 0.6% (wt.%) by weight of cement. As Figure 7 shows, the compressive strength of the mortar sample evidently decreases at SPP concentration of 1.2% and 2.4% by weight of cement. Shi et al. [14] proposed that the excessive insoluble substances in mortar pores may lead to the expansion and the cracking of internal micro-structure. Therefore, in the present study, as the results in figures 6a and figure 7 shows, the excessive addition of SPP in the mortar would act as retarder and reduces the strength of mortars, which could reduce the barrier effect to chloride ion and decrease its inhibition efficiency. However, as concluded by Feng [24] and Morris [43], the concrete/rebar interfacial condition is the major factor of the corrosion initiation of rebars, which is more significantly than the concrete cover layer. Thus, the excessive addition of SPP enhances the permeability of mortar cover layer, resulting in the acceleration of the migration of aggressive ions (Cl^-) and enhancement the corrosion rate of rebars in the chloride containing mortar. Simultaneously, the adsorbed layer formed on the steel surface by the addition of SPP in chloride contaminated mortar plays the critical role to retard the corrosion. Therefore, SPP can be used as an effective corrosion inhibitor in chloride-containing mortar. The most suitable content of SPP is 0.6% (wt.%), which concurs with the conclusions of OCP and LPR.

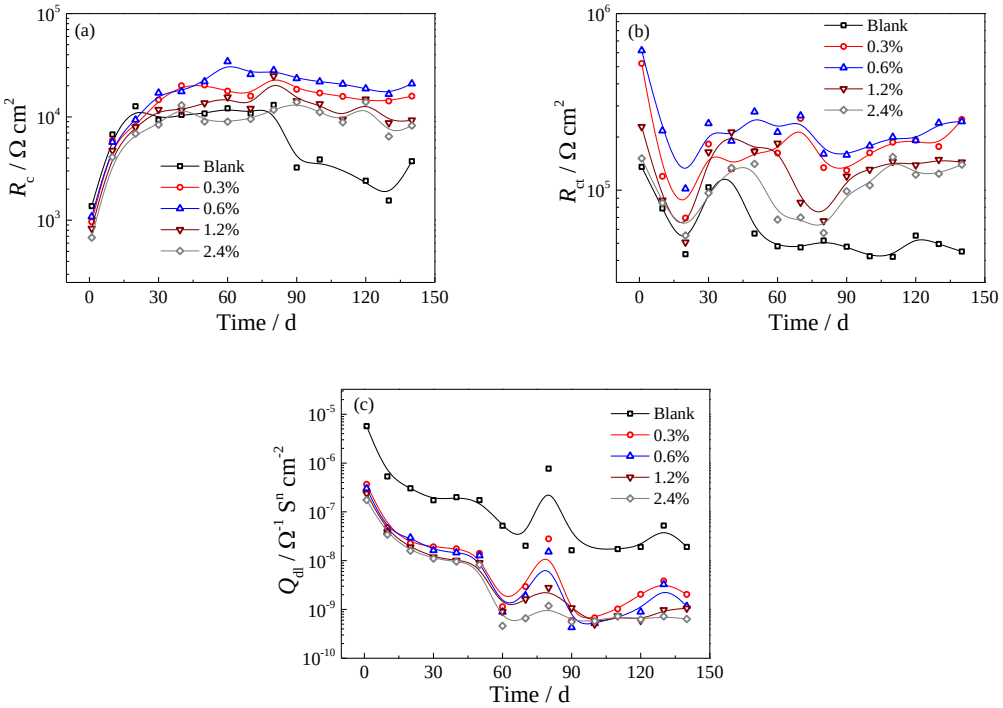

Figure 6. Variation of EIS fitting results for the rebars in chloride contaminated mortar with different contents of SPP. (a) R_c, (b) R_{ct}, (c) Q_{dl}.

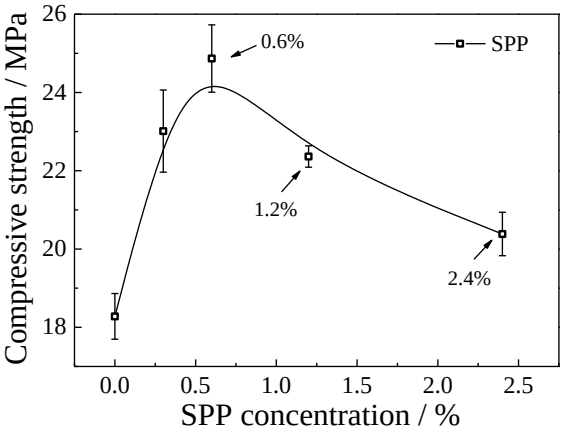

Figure 7. Variation of compressive strength of the chloride contaminated mortar at 14 d with different contents of SPP.

3.4 Potentiodynamic polarization

At 120 days, the polarization curves of the rebars in the chloride contaminated mortar with different contents of SPP are tested and the results are shown in figure 8. The corrosion parameters were analyzed by Corrview software and the results are presented in Table 1. The inhibition efficiency η (%) of SPP is calculated by Eq. (6) [46, 47].

$$\eta\ (\%) = \frac{i_{corr-abs} - i_{corr-pres}}{i_{corr-abs}} \times 100 \qquad (6)$$

where the $i_{corr\text{-}pres}$ and $i_{corr\text{-}abs}$ are the corrosion current density of rebars in mortar with and without

SPP, respectively obtained from the polarization curves fitted results. The i_{corr} is in the magnitude of 10^{-7}~10^{-6} A cm^{-2}, which is consistent with the corrosion current densities results from polarization resistance (figure 2). Clearly, the i_{corr} of the steel samples in mortar containing SPP are lower than that of the one in mortar without SPP. The corrosion potentials (E_{corr}) of the steel samples were enhanced by the the addition of SPP. According to literatures [16, 48], this results indicate that the SPP is a classical anodic corrosion inhibitor for carbon steel in the chloride contaminated mortar. As the results of η in Table 1 show, the corrosion of the rebars is evidently inhibited by the addition of SPP in chloride contaminated mortar. When the content of SPP is 0.6% (wt.%) by the weight of cement, the corrosion inhibition efficiency almost reaches 90%, which is the highest. It can be concluded that the SPP can effectively hinder the corrosion of steel bars in the chloride contaminated mortar. The corrosion potential (E_{corr}) of steel sample in mortar with SPP of 0.6% by weight of cement also is the highest, but it decreased as the contents of SPP further increased. In line with the results of OCP, LPR and EIS measurements, the situation suggests that the most suitable contents of SPP in the mortar is 0.6% by weight of cement, and the excessive addition could decrease its inhibition efficiency.

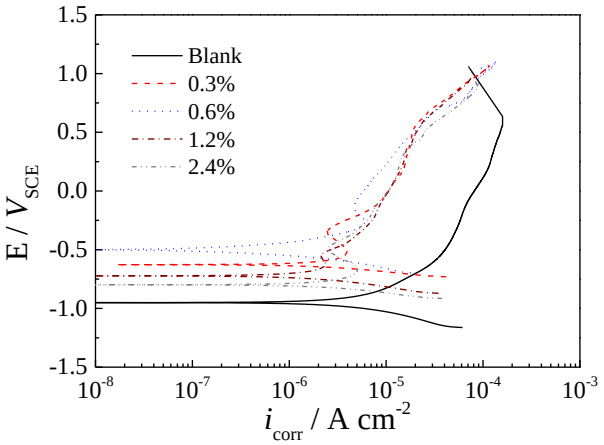

Figure 8. Polarization curves of carbon steel bars in the chloride contaminated mortar with different concentrations of SPP at 120 d.

Table 1. Electrochemical parameters of carbon steel bars in the chloride contaminated mortar with different concentrations of SPP at 120 d.

SPP concentration (%)	E_{corr} (V_{SCE})	i_{corr} (A/cm^2)	η (%)	σ_{corr} (mm/y)
Blank	-0.95	9.778×10^{-7}	—	0.0110
0.3	-0.63	2.124×10^{-7}	78	0.0016
0.6	-0.50	1.032×10^{-7}	89	0.0012
1.2	-0.72	4.105×10^{-7}	58	0.0047
2.4	-0.80	5.320×10^{-7}	46	0.0059

3.5 Corrosion state and surface characterization of carbon steel bar

After 90 days immersion, the corrosion state of the rebars in chloride contaminated mortar was

examined after the potentiodynamic polarization measurements, and the results are shown in figure 9. As the photographs show, the steel bars in mortar without SPP are evidently corroded (figure 9a), and the corrosion products mostly distribute in the middle part of the rebar. Figure 6a shows that the R_c of steel bar in the mortar without SPP significantly decreases after 90 days. It could be attributed to the micro-cracks formed inside the mortar cover layer caused by the rust expansion of the steel bar. For the steel samples embedded in the SPP-containing mortar (figures 9b~9e), the corrosion of rebars is obviously inhibited, obvious less rusts are visible on the steel surface. Especially, almost no corrosion products can be observed on the steel surface in mortar with 0.6% SPP, while the corrosion of steel bar embedded in mortar with 1.2% and 2.4% SPP are severer. The results in figure 9 directly confirm that the SPP can effectively inhibit the corrosion of rebars in the chloride contaminated mortar, and the excessive SPP addition could decrease its inhibition efficiency, while the most suitable concentration is 0.6% by weight of cement.

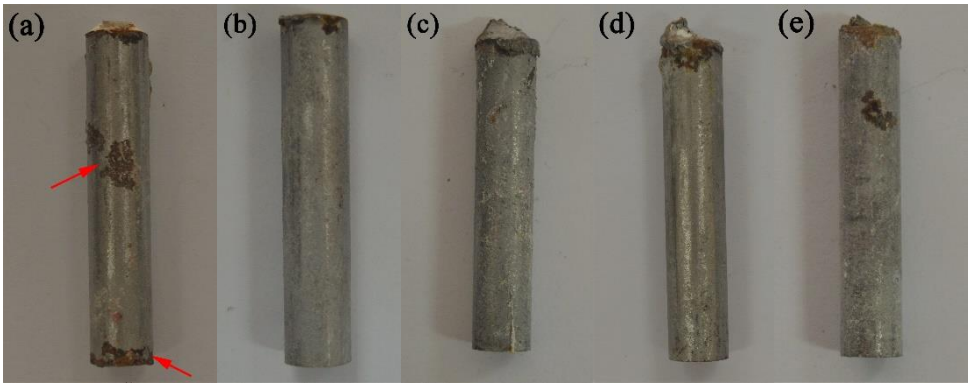

Figure 9. Photographs of carbon steel samples in chloride contaminated mortar with different concentrations of SPP at 90 d. (a) 0%, (b) 0.3%, (c) 0.6%, (d) 1.2%, (e) 2.4%.

After being immersed 48 h, the surface of steel samples in the simulated concrete pore solution with different contents of SPP was observed by using scanning electron microscope, and the results are shown in figure 10. Obviously, the surface of steel immersed in solution containing SPP is much smoother, and no obvious corrosion products due to the phosphate protective films. According to Eq. (5) and the results in figure 6 c, the thickness of the protective films increases with SPP concentration, which can further be confirmed by figures 10 b~10 e, where the steel surface become smoother as the content of SPP increased in the pore solution. The results revealed that the SPP can effectively inhibit the steel corrosion, and the inhibition effect increased with the concentration of SPP in simulated concrete pore solution, which concurs with the results of Q_{dl} (figure 6c). On the other hand, this situation together with the results of R_c (figure 6a) and compressive strength (figure 7), furtherly confirm that the corrosion inhibition efficiency decreases when the contents of SPP exceeds 0.6% by weight of cement could be ascribed to the increasing defects in the concrete cover layer, which accelerates the permeation of chloride ions into the mortars.

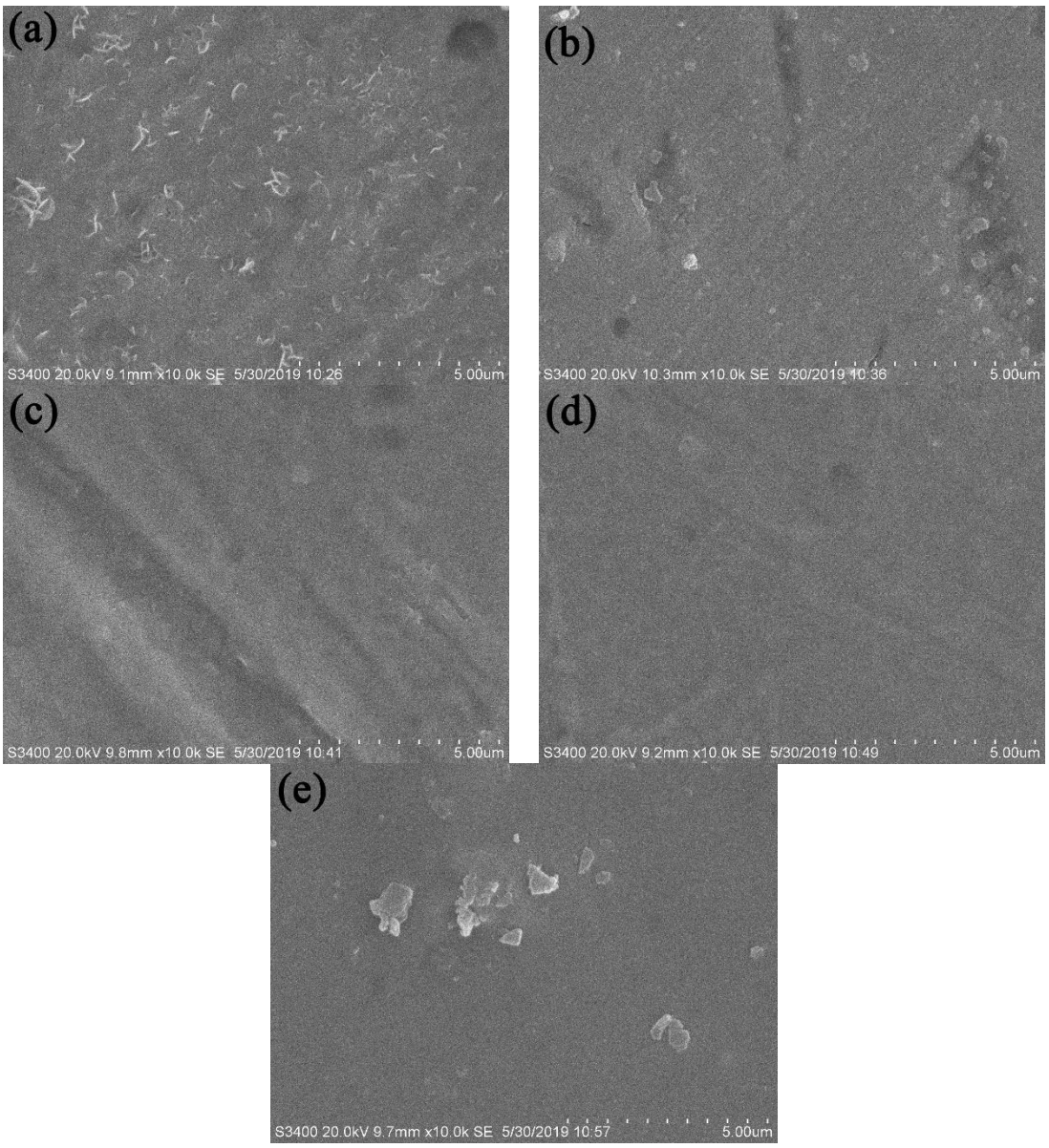

Figure 10. SEM of the carbon steel bars after 48 h immersion in the simulated concrete pore solution with different concentrations of SPP. (a) 0%, (b) 0.3%, (c) 0.6%, (d) 1.2%, (e) 2.4%.

4. CONCLUSIONS

In the present study, different concentrations of SPP were used to inhibit the corrosion of the Q235 carbon steel bar in the chloride-contaminated mortars. The corrosion inhibition efficiency was investigated via OCP, LPR, and EIS tests, respectively. The following conclusions can be drawn from the results：

1. The values of OCP, polarization resistance, as well as the impedances of carbon steel rebars in mortar were significantly increased, while the corrosion current density was reduced by the addition of SPP, which suggests that the corrosion of the reinforcing steel was hindered by SPP.

2. SPP was categorized an anodic corrosion inhibitor, owing to it enhanced the corrosion potential and decreased the corrosion current density of the carbon steel in the chloride contaminated mortar. The pores in the mortar were blocked by the phosphate products from the reaction between cement and the hydrolysis products of SPP, which reduces the mortar porosity and hindered the permeation of chloride in the solution. The increasing of Q_{dl} suggested an absorb films formed on the surface of the carbon steel, and the layer became thicker as the SPP concentration increased, which protected the steel bar from corrosion.

3. When the content of SPP in the mortars was 0.6% by weight of cement, the corrosion current density (i_{corr}) of the carbon steel was the lowest, and the inhibition efficiency (η) of SPP was the highest. Thus, the suitable content of the SPP in the chloride-containing mortar was proposed at 0.6% by weight of cement.

4. As the contents of SPP exceeded the proposed dosage, the excessive addition of SPP decreased the compactness of the mortar layer and accelerated the permeation of chloride into the mortar, then the corrosion rate of reinforcing steel was increased and its inhibition efficiency was decreased by the excessive SPP.

ACKNOWLEDGEMENTS
This research was funded by the National Natural Science Foundation of China (51601074), the Fundamental Research Funds for the Central Universities (2018B07214, 2018B56714), the Opening Fund of State Key Laboratory of Geohazard Prevention and Geoenvironment Protection (Chengdu University of Technology) (Grant SKLGP2017K011, SKLGP2018K014).

References

1. M. Manera, O. Vennesland and L. Bertolini, *Corros. Sci.*, 50 (2008) 554.
2. W. Zhang, Y. Cao and Y.L. Zhu, *J. Hydrol.*, 564 (2018) 588.
3. X.G. Feng, Y.W. Xu, X.Y. Zhang, X.Y. Lu, L.Y. Zhang, R.L. Shi, J. Zhang, D. Chen and X.B. Zhang, *Int. J. Electrochem. Sci.*, 13 (2018) 10339.
4. L. Dhouibi, E. Triki and A. Raharinaivo, *Cem. Concr. Comp.*, 24 (2002) 35.
5. J.J. Shi, W. Sun, *Int. J. Min. Met. Mater.*, 19 (2012) 38.
6. S.N. Berke, M.C. Hicks, *Cem. Concr. Compos.*, 26 (2004) 191.
7. X.G. Feng, Y.M. Tang, X.H. Zhao and Y. Zuo, *J. Wuhan Univ. Technol. Mater. Sci. Ed.*, 27 (2012) 994.
8. M.P.S. Chandrawat, R.N. Yadav, *Bull. Mater. Sci.*, 23 (2000) 69.
9. L. Mandecka-Kamień, W. Kurdowski, *Cem.-Lime-Concr.*, 16 (2011) 355.
10. H. Nahali, L. Dhouibi and H. Idrissi, *Constr. Build. Mater.*, 78 (2015) 92.
11. C. Alonso, C. Andrade, C. Argiz and B. Malric, *Cem. Concr. Res.*, 26 (1996) 405.
12. T. Chaussadent, V. Nobel-Pujol, F. Farcas, I. Mabille and C. Fiaud, *Cem. Concr. Res.*, 36 (2006) 556.
13. A.L. Iglesia, V.M.L. Iglesia, S. Fajardo, P.P. Gómez and J.M. Bastidas, *Constr. Build. Mater.*, 37 (2012) 46.
14. J.J. Shi, W. Sun, *Cem. Concr. Comp.*, 45 (2014) 166.
15. L. Yohai, M.B. Valcarce and M. Vázquez, *Electrochim. Acta*, 202 (2016) 316.
16. L. Yohai, W. Schreinerb, M. Vázquez and M.B. Valcarce, *Electrochim. Acta*, 202 (2016) 231.
17. D.M. Bastidas, M. Criado, V.M.L. Iglesia, S. Fajardo, A.L. Iglesia and J.M. Bastidas, *Cem. Concr. Comp.*, 43 (2013) 31.

18. D.M. Bastidas, M. Criado, S. Fajardo, A.L. Iglesia and J.M. Bastidas, *Cem. Concr. Comp.*, 61 (2015) 1.
19. S. Chen, L.H. Jiang, J.X. Xu, L.S. You and T. Wang, *Corrsion & Protection*, 33 (2012) 5. (in Chinese)
20. N. Etteyeb, L. Dhouibi, M. Sanchez, C. Alonso, C. Andrade and E. Triki, *J. Mater. Sci.*, 42 (2007) 4721.
21. V.K. Gouda, W.Y. Halaka, *Brit. Corros. J.*, 5 (1970) 204.
22. L. Mammolitia, C.M. Hanssona and B.B. Hope, *Cem. Concr. Res.* , 29 (1999) 1583.
23. X.G. Feng, X.Y. Lu, Y. Zuo, N. Zhuang and D. Chen, *Corros. Sci.*, 103 (2016) 223.
24. X.G. Feng, X.Y. Lu, Y. Zuo, N. Zhuang and D. Chen, *Corros. Sci.*, 103 (2016) 66.
25. S.G. Dong, B. Zhao, C.J. Lin, R.G. Du, R.G. Hu and G.X. Zhang, *Constr. Build. Mater.*, 28 (2012) 72.
26. B.M. Fan, H. Hao, B. Yang and Y. Li, *Res. Chem. Intermed.*, 44 (2018) 5711.
27. N. Gartner, T. Kosec and A. Legat, *Mater. Chem. Phys.*, 184 (2016) 34.
28. X.F. Huang, G.M. Han and W.G. Huang, *Mater.*, 11 (2018) 628.
29. F.E.T. Heakal, A.M. Fekr and M.Z. Fatayerji, *Electrochim. Acta*, 54 (2009) 1545.
30. ASTM C 349. Standard test method for compressive strength of hydraulic-cement mortars *American Society for Testing and Materials* 2014, Philadelphia.
31. L.M. Grover, U. Gbureck, A.M. Young, A.J. Wrightd and J.E. Barralet, *J. Mater. Chem.*, 15 (2005) 4955.
32. ASTM G 59-97. Standard test method for conducting potentiodynamic polarization resistance measurements. *American Society for Testing and Materials* 2014, Philadelphia.
33. M. Stern, A.L. Geary, *J. Electrochem. Soc.*, 104 (1957) 55.
34. C. Alonso, C. Andrade and J.A. González, *Cem. Concr. Res.*, 18 (1988) 687.
35. C. Andrade, C. Alonso, *Constr. Build. Mater.*, 10 (1996) 315.
36. J.M. Miranda, A.F. Jiménez, J.A. González and A. Palomo, *Cem. Concr. Res.*, 35 (2005) 1210.
37. M.O.G.P. Braganc, K.F. Portell, M.M. Bonato and C.E.B. Marino, *Constr. Build. Mater.*, 68 (2014) 650.
38. C. Andrade, M. Keddam, X.R. Novoa, M.C. Perez, C.M. Rangel and H. Takenouti, *Electrochim. Acta*, 46 (2001) 3905.
39. A.A. Gürten, K. Kayakırılmaz and M. Erbil, *Constr. Build. Mater.*, 21 (2007) 669.
40. J.M. Deus, B. Díaz, L. Freire and X.R. Nóvoa, *Electrochim. Acta*, 131 (2014) 106.
41. C.H. Hsu, F. Mansfeld, *Corros.*, 57 (2001) 747.
42. S. Gadadhar, R. Balasubramaniam, *Corros. Sci.*, 50 (2008) 131.
43. W. Morris, A. Vico and M. Vazquez, *J. Appl. Electrochem.*, 33 (2003) 1183.
44. S.K. Sarkar, B.Y. Lee, A.R. Padalhin and A. Sarker, *J. Biomater. Appl.*, 30 (2015) 823.
45. S. Meininger, C. Blum, M. Schamel, J.E. Barralet, A. Ignatius and U. Gbureck, *Sci. Rep.*, 7 (2017) 558.
46. S.X. Zheng, W. Zhang, M. Li and L.Y. Gong, *Corros. Sci.*, 95 (2015) 168.
47. B.M. Fan, G. Wei, Z. Zhang and N. Qiao, *Corros. Sci.*, 83 (2014) 75.
48. M.J. Pryor, M. Cohen, *J. Electrochem. Soc.*, 5 (1953) 203.

© 2019 The Authors. Published by ESG (www.electrochemsci.org). This article is an open access article distributed under the terms and conditions of the Creative Commons Attribution license (http://creativecommons.org/licenses/by/4.0/).